

Animal Re-Identification on Microcontrollers

Yubo Chen

University of Auckland
Auckland, New Zealand
ych259@aucklanduni.ac.nz

Di Zhao

University of Auckland
Auckland, New Zealand
di.zhao@auckland.ac.nz

Yun Sing Koh

University of Auckland
Auckland, New Zealand
y.koh@auckland.ac.nz

Talia Xu

University of Auckland
Auckland, New Zealand
talia.xu@auckland.ac.nz

Abstract

Camera-based animal re-identification (Animal Re-ID) can support wildlife monitoring and precision livestock management in large outdoor environments with limited wireless connectivity. In these settings, inference must run directly on collar tags or low-power edge nodes built around microcontrollers (MCUs), yet most Animal Re-ID models are designed for workstations or servers and are too large for devices with small memory and low-resolution inputs. We propose an on-device framework. First, we characterise the gap between state-of-the-art Animal Re-ID models and MCU-class hardware, showing that straightforward knowledge distillation from large teachers offers limited benefit once memory and input resolution are constrained. Second, guided by this analysis, we design a high-accuracy Animal Re-ID architecture by systematically scaling a CNN-based MobileNetV2 backbone for low-resolution inputs. Third, we evaluate the framework with a real-world dataset and introduce a data-efficient fine-tuning strategy to enable fast adaptation with just three images per animal identity at a new site. Across six public Animal Re-ID datasets, our compact model achieves competitive retrieval accuracy while reducing model size by over two orders of magnitude. On a self-collected cattle dataset, the deployed model performs fully on-device inference with only a small accuracy drop and unchanged Top-1 accuracy relative to its cluster version. We demonstrate that practical, adaptable Animal Re-ID is achievable on MCU-class devices, paving the way for scalable deployment in real field environments.

ACM Reference Format:

Yubo Chen, Di Zhao, Yun Sing Koh, and Talia Xu. 2025. Animal Re-Identification on Microcontrollers. In *Proceedings of Conference*

Permission to make digital or hard copies of all or part of this work for personal or classroom use is granted without fee provided that copies are not made or distributed for profit or commercial advantage and that copies bear this notice and the full citation on the first page. Copyrights for components of this work owned by others than the author(s) must be honored. Abstracting with credit is permitted. To copy otherwise, or republish, to post on servers or to redistribute to lists, requires prior specific permission and/or a fee. Request permissions from permissions@acm.org. *Conf '25, Location*

© 2025 Copyright held by the owner/author(s). Publication rights licensed to ACM.

ACM ISBN 978-1-4503-XXXX-X/25/XX
<https://doi.org/XXXXXXX.XXXXXXX>

Name (Conf '25). ACM, New York, NY, USA, 14 pages. <https://doi.org/XXXXXXX.XXXXXXX>

1 Introduction

Tracking specific individual animals is central to many real-world applications. In wildlife management, for example, reliably re-identifying individuals is essential for monitoring pest populations or protecting endangered species. However, doing so manually is often labour-intensive and error-prone. Animal Re-identification (Animal Re-ID) automates this process by recognising animals across varying times, environments, and viewpoints [22]. This capability converts isolated sightings into reliable data for population assessment and targeted interventions [12]. Implementing reliable Animal Re-ID in real-world scenarios, however, is difficult. Animal Re-ID must distinguish between specific, often similar-looking individuals. To achieve this, state-of-the-art (SOTA) methods rely on large machine learning architectures like vision transformers and vision-language models [26]. The large number of parameters needed to capture these differences results in high computational costs and memory footprints, limiting their deployment to powerful servers or workstations [1, 35, 51].

This hardware limitation imposes a disconnect between where data is collected and where it is processed. While field devices like camera traps record images in the wild, they lack the capacity to analyse them locally (due to the large model size). This means personnel has to offload data to central servers for analysis, which is a slow process that becomes a major bottleneck in remote areas. Without network coverage, data retrieval often requires manually collecting SD cards. Even where connectivity exists, transmitting the sheer volume of raw images creates significant delays and costs [37, 43]. This latency prevents field researchers from accessing the real-time insights needed to adjust strategies or deploy resources effectively [23].

To address these connectivity and bandwidth issues, we aim to enable Animal Re-ID directly on edge devices. We propose a lightweight Animal Re-ID framework designed for microcontrollers (MCUs), which is able to fit within memory limits while maintaining high accuracy. This enables low-latency, autonomous recognition without relying on continuous connectivity. Figure 1 illustrates this operation flow compared to a cloud-based inference. Realising this on-device solution presents a dual challenge on memory

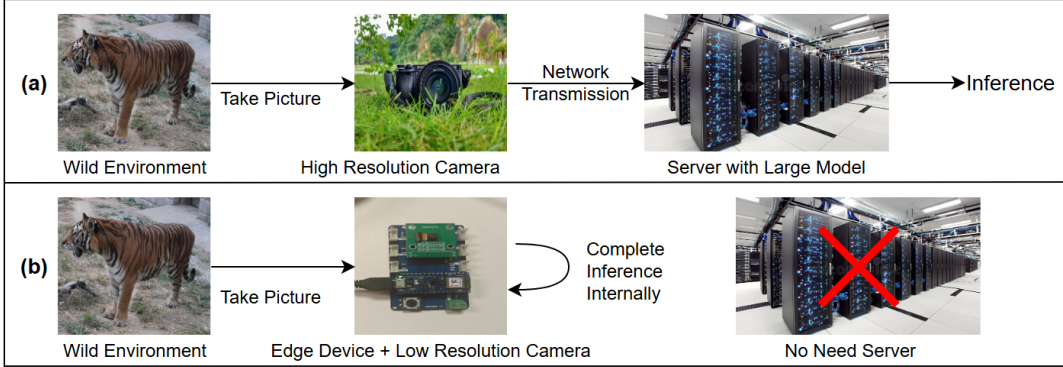


Figure 1: Comparison of Animal Re-Identification workflows. (a) Traditional cloud-based pipeline, where captured images are uploaded to a remote server for feature extraction and identification. (b) Our proposed MCU-based on-device pipeline, which performs end-to-end inference locally and outputs individual IDs without relying on cloud computation.

limits and input quality. The first is the resource gap: while SOTA Animal Re-ID models typically require hundreds of megabytes to capture complex features, standard MCUs typically have less than 1 MB of onboard memory [14, 34]. This makes it physically impossible to store standard architectures on the MCUs. The second challenge is the input quality gap: edge devices often use low-resolution cameras that cannot capture the fine details found in high-quality camera trap datasets, due to cost and power constraints [29, 37]. The core research problem of this project, therefore, is to design a model that is sufficiently compact to fit on an MCU, but also robust enough to reliably identify individual animals from low-quality, degraded images at the same time. In this work, we systematically investigate the design of Animal Re-ID models capable of running directly on MCU-class hardware. Our contributions are as follows:

Contribution 1 [Section 3]: Investigating the limits of knowledge distillation. We first investigate whether knowledge distillation, teaching a small model to mimic a large one, is sufficient to bridge the gap between server-grade performance and MCU constraints. Our experiments show that this approach leads to diminishing returns. When the architectural gap is large and inputs are low-resolution, the tiny “student” model struggles to capture the complex representations of the “teacher” model. This indicates that standard transfer learning alone is insufficient for edge hardware, motivating a shift toward direct structural redesign.

Contribution 2 [Section 4]: Optimising model structure for low-resolution inputs. We perform a systematic study to understand how model structure affects identification performance on resource-constrained hardware. By analysing channel width and network depth, we characterise the trade-off between memory footprint and accuracy. Our results demonstrate that for degraded edge images (64×64),

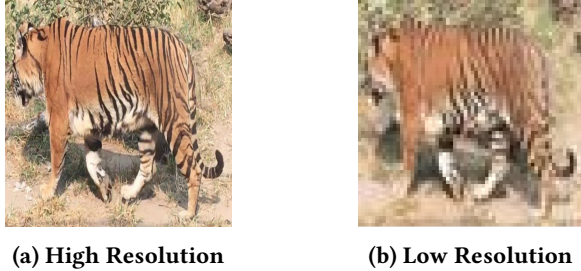
deep feature extraction is redundant. This allows us to truncate a significant portion of the network layers and identify a compact configuration that is both robust and efficient.

Contribution 3 [Section 5]: Empirical validation of on-device feasibility. We provide a proof-of-concept system for end-to-end Animal Re-ID running entirely on an Arduino Nano 33 BLE Sense. Through field evaluation with a real-world cattle dataset, we demonstrate that our optimised model delivers reliable inference despite the noise of edge hardware. Furthermore, we introduce a data-efficient adaptation strategy, showing that the device can be efficiently fine-tuned to recognise new animals in new environments using only a few samples, effectively closing the loop between efficient design and field deployment.

2 System Constraints and Setup

2.1 Hardware Constraints

To make Animal Re-ID practical for widespread deployment, the hardware must be compact, affordable, and energy-efficient. We target the Arduino Nano 33 BLE Sense as a representative platform for embedded Animal Re-ID applications. This device offers a standard, widely accessible configuration for milliwatt-range edge processing: it has 1 MB of Flash (about 960 KB usable by the application) and 256 KB of SRAM. This avoids the high power consumption of Single-Board Computers (such as the Raspberry Pi), which typically require watt-level power, while providing more resources than extreme ultra-low-power sensors (often < 64 KB memory) that cannot buffer a single image frame. However, these resources are still very limited for deep learning. Buffering a single high-resolution image ($1920 \times 1080 \times 3$ pixels, 8-bit) would require over 6 MB of memory, far exceeding the available 256 KB of SRAM, so the system is physically restricted to processing low-resolution inputs.



(a) High Resolution

(b) Low Resolution

Figure 2: Comparison between high-resolution and low-resolution sample images in the ATRW dataset

To characterise the input quality expected within this power budget, we use the OV7675 CMOS module as an example. While this camera is widely used with Arduino, it introduces a severe quality gap compared to standard datasets: as shown in Figure 2, the raw output suffers from visible noise, colour distortion, and limited dynamic range. To ensure our model is robust to these deployment realities, we explicitly align our experimental data with these physical limits. All training and evaluation images are down-sampled to $64 \times 64 \times 3$, which corresponds to roughly 12 KB per frame (vs. > 6 MB for $1920 \times 1080 \times 3$), so that both the input and the intermediate activations fit comfortably within a 120 KB TensorFlow Lite Micro tensor arena on the 256 KB SRAM. On the Flash side, after reserving space for program code and gallery embeddings, we estimate that only about 600–700 KB of the 960 KB user-accessible Flash can be devoted to the Animal Re-ID model. These constraints motivate the model compression explored in the following sections.

2.2 Animal Datasets

We develop and evaluate our framework using two complementary types of data: public benchmarks to assess generalisation across diverse species, and a custom field-collected dataset to validate the full deployment pipeline in a real-world setting.

Public Benchmark Datasets. We use six publicly available datasets: ATRW, FriesianCattle2017, LionData, MPDD, iPanda50, CoBRA ReID Youngstock [4, 8, 13, 25, 31, 45]. These datasets create a comprehensive benchmark covering a wide variety of species, including tigers, pandas, lions, cattle, and dogs. This diversity allows us to evaluate our model’s ability to generalise across different animal patterns and imaging conditions, ranging from controlled enclosures to wild environments with complex backgrounds.

Real-World Deployment Dataset. To validate the model’s performance in a target edge environment, we collect a local cattle Re-ID dataset in Auckland, New Zealand. This dataset presents a distinct visual setting from public benchmarks and creates a potential “reality gap”: high accuracy on standard datasets may not translate to this specific farm due to unseen breeds, lighting, and backgrounds. To evaluate

this risk under practical constraints, we simulate a “rapid deployment” scenario. Since collecting thousands of training images per site is infeasible, we do not perform full-scale training. Instead, we provide the model with only a handful of reference images per animal, testing its ability to adapt to new individuals in an unfamiliar environment with minimal setup data.

Dataset Organisation. We divide each dataset into three subsets that mirror the stages of a real-world deployment. The Training Set is used offline to teach the model, allowing it to learn the unique visual patterns required to distinguish one individual from another. The Gallery Set acts as the on-device database. These images are the “registered” templates for known animals. Finally, the Query Set represents new, unidentified sightings captured in the field. When the device takes a photo, it treats it as a query, comparing it against the stored Gallery to find the matching identity.

3 Initial Study

A natural approach for achieving high Animal Re-ID accuracy under tight resource constraints is to start with an existing well-performed model and make it smaller, rather than designing small architectures from scratch. Knowledge distillation is a widely used technique for this purpose: a large *teacher* model is first trained to produce high-quality features, and a smaller *student* model is then trained to mimic the teacher while trying to preserve most of its accuracy [15, 28]. Therefore, it is a natural candidate to obtain compact Animal Re-ID models suitable for MCU deployment.

3.1 Teacher and Student Models

We choose two different backbones for our teacher and student models, one CNN and the other vision transformer (ViT) based, covering the two main vision model families used in practice. Out of the two types of models, CNNs remain the most practical choice for MCU deployment, whereas Vision Transformers have become a standard backbone for large, pre-trained vision systems. Combining these two families allows us to separate three factors that influence distillation under MCU constraints: (i) model size, (ii) architecture family (CNN vs. Transformer), and (iii) low-res image inputs.

T1: ViT-based teacher model: CLIP-ReID [26]. CLIP is trained on large-scale image–text pairs and thus provides visual features with strong cross-domain generalisation [32]. CLIP-ReID introduces ID-specific learnable text tokens and a two-stage training scheme that aligns all images of the same identity with a shared text prototype [26], yielding features that are robust to changes in viewpoint, illumination and background.

T2: CNN-based teacher model: Few-Shot Animal Re-ID [44]. By combining transfer learning with few-shot training, the Few-Shot model can learn useful embeddings from only a

handful of images per individual and works across diverse species without customisation [44].

S1: CNN-based student model: MobileNetV2 [36]. MobileNetV2 is a compact CNN originally designed for mobile and other resource-constrained devices [36]. It offers a good balance between accuracy and efficiency on standard vision benchmarks and has been successfully deployed in multiple embedded, on-device vision applications [3].

S2: ViT-based student model: ViT-Tiny [41]. ViT-Tiny is a small Vision Transformer that follows the same overall design as our ViT-based teacher T1 [9, 10, 41]. Although ViT-Tiny is less hardware-friendly than MobileNetV2 on current MCUs, it gives us a compact ViT-based model to separate the effect of model size from the effect of architecture in distillation.

These models allow us to answer two questions: when is distillation a useful route toward MCU-ready Animal Re-ID, and which combinations of teacher-student model offer the best balance between accuracy and edge deployability?

3.2 Knowledge Distillation

In our knowledge distillation experiments, we study three variants: ViT → CNN, ViT → ViT, and CNN → CNN. The dataset is split following the steps described in Section 2. Each model is evaluated on six public Animal Re-ID datasets, reporting mean Average Precision (mAP) and Rank-1, Rank-5, and Rank-10 retrieval accuracy. mAP measures how well the model retrieves all correct matches in the gallery [50].

3.2.1 Transformer-to-CNN (T1 → S1). We first fine-tune CLIP-ReID on each Animal Re-ID dataset using the procedure of [26]. For every training image, the teacher produces an embedding, a vector that summarises the appearance of the individual. The student model is trained to match these embeddings between the teacher and student features, as well as to predict the correct identity with a standard cross-entropy loss on its class predictions. The final training objective is a weighted sum of these two terms. For this comparison, we look at the Clip-ReID teacher (T1), the distilled MobileNetV2 student (S1), and a MobileNetV2 model (blue) trained directly on each dataset without distillation. in Table 1.

Across datasets, the directly trained MobileNetV2 achieves comparable performance to the teacher model despite being $\sim 40\times$ smaller (477 MB vs. 12 MB). On the other hand, feature-level distillation from the ViT-based CLIP-ReID teacher (T1) to the MobileNetV2 student (S1) on Animal Re-ID benchmarks fails to improve the student model. On most datasets, the distilled student achieves lower mAP and Rank- k accuracy than the same MobileNetV2 without distillation. This suggests that forcing a CNN to reproduce ViT embeddings via a simple MSE loss is a poor fit, likely because the two

architectures encode visual information with very different inductive biases, a challenge also noted in earlier work [2]. These results motivate a second distillation setup in which the student architecture is closer to the CLIP-ReID teacher.

3.2.2 Transformer-to-Transformer (CLIP-ReID (T1) → ViT-Tiny (S2)). To reduce the architectural mismatch seen above, we next adopt ViT-Tiny as a Transformer-based student. We consider two feature-level distillation methods: ViTKD [48] and TeKAP [16], both of which train a smaller ViT to align its internal features with those of a larger teacher. We also train a plain ViT-Tiny baseline without distillation, so that any performance differences can be attributed to distillation rather than simply switching to a ViT-based model.

Table 2 shows the results for the CLIP-ReID teacher, the non-distilled ViT-Tiny student, and its ViTKD- and TeKAP-distilled variants. The plain ViT-Tiny performs similarly to the teacher model, while the ViTKD- and TeKAP-distilled ViT-Tiny students achieve teacher-level retrieval performance using a substantially smaller Transformer. This shows that once the student shares the teacher’s Transformer architecture, feature-level distillation can effectively compress the teacher model without losing much accuracy, and that the poor results in the Transformer-to-CNN setting are largely due to architectural mismatch rather than an inherent limitation of distillation.

However, when we turn from accuracy to deployment, Transformer-based students introduce a different challenge: even this reduced model remains too large for our target device. Our S2 is roughly 22 MB in size, which is roughly 1.8 times larger than S1 far above the memory budget of MCUs. Because self-attention compares every image patch with every other patch across multiple layers, ViT models require a minimum hidden size and number of attention heads to preserve the global interactions that make them effective. Pushing these dimensions much lower leads to sharp drops in accuracy [24]. Thus, Transformer-to-Transformer distillation resolves the architectural-mismatch problem and yields a compact ViT with teacher-level performance, but it is difficult to meet the memory constraints of MCU hardware. These constraints motivate us to focus back on CNN-based students, but now with a CNN teacher to avoid the architectural mismatch observed in the CLIP-ReID → MobileNetV2 experiments.

3.2.3 From Few-Shot (T2) to CNN Student Model (S1). After observing that distillation from the ViT-based CLIP-ReID teacher to a MobileNetV2 student yielded only limited gains, we hypothesise that the large architectural gap between a transformer teacher and a lightweight CNN student hinders effective knowledge transfer. We therefore choose a conventional CNN-based animal Re-ID framework, rather than

Table 1: Performance comparison for T1 → S1

Method	ATRW				FriesianCattle2017				LionData			
	mAP	Top-1	Top-5	Top-10	mAP	Top-1	Top-5	Top-10	mAP	Top-1	Top-5	Top-10
CLIP-ReID	58.2	94.6	98.6	99.3	89.0	97.6	100.0	100.0	23.9	29.5	68.9	86.9
MobileNetV2 ¹	40.6	88.2	95.5	97.4	85.0	92.9	100.0	100.0	23.4	24.6	67.2	80.3
MobileNetV2 ²	51.2	90.6	96.9	98.6	95.3	100.0	100.0	100.0	35.7	42.6	80.3	86.9

¹ MobileNetV2 distilled from CLIP-ReID. ² Trained without distillation.

Table 2: Performance comparison for T1 → S2.

Method	ATRW				FriesianCattle2017				LionData			
	mAP	Top-1	Top-5	Top-10	mAP	Top-1	Top-5	Top-10	mAP	Top-1	Top-5	Top-10
CLIP-ReID	58.2	94.6	98.6	99.3	89.0	97.6	100.0	100.0	23.9	29.5	68.9	86.9
ViT-Tiny ¹	53.8	94.6	98.1	98.6	92.6	100.0	100.0	100.0	33.9	49.2	80.3	86.9
ViT-Tiny ²	55.4	95.8	98.6	99.5	94.4	100.0	100.0	100.0	35.2	44.3	80.3	88.5
ViT-Tiny ³	53.1	94.6	98.1	98.6	84.3	96.5	98.8	98.8	34.6	49.2	78.7	88.5

¹ ViT-Tiny distilled from CLIP-ReID using ViTKD. ² ViT-Tiny distilled from CLIP-ReID using TeKAP. ³ Trained without distillation.

Table 3: Performance comparison for T2 → S1.

Method	ATRW				FriesianCattle2017				LionData			
	mAP	Top-1	Top-5	Top-10	mAP	Top-1	Top-5	Top-10	mAP	Top-1	Top-5	Top-10
Few-Shot	45.5	87.5	96.5	98.1	84.6	91.8	100.0	100.0	20.3	21.3	53.7	72.1
MobileNetV2 ¹	50.0	87.7	95.5	96.9	90.9	95.3	100.0	100.0	21.1	31.1	55.7	63.9
MobileNetV2 ²	51.2	90.6	96.9	98.6	95.3	100.0	100.0	100.0	35.7	42.6	80.3	86.9

¹ MobileNetV2 distilled from Few-Shot. ² Trained without distillation.

the CNN variant of CLIP-ReID, to isolate the effect of architectural compatibility between the CNN teacher and the MobileNetV2 student without reintroducing CLIP’s multi-modal machinery. In this CNN-to-CNN distillation setting, we adopt the Few-Shot Animal Re-ID framework [44] as our teacher model (T2), whose backbone is a CNN-based DenseNet-121 network. As shown in Table 3, the directly trained MobileNetV2 consistently achieves higher mAP and Top- K identification accuracy than the Few-Shot teacher, indicating that the teacher does not provide a stronger representation than this lightweight CNN baseline.

These results show that, for the Animal Re-ID task, the Few-Shot model does not provide a stronger representation than a directly trained MobileNetV2. Few-Shot is designed for episodic, low-shot recognition across tasks and is trained with a metric-learning objective geared toward rapid adaptation from very few examples. In contrast, our MobileNetV2 baseline is trained directly on each animal Re-ID dataset with all available identity labels and is evaluated on repeated retrieval of the same individuals. More generally, our findings show that when the teacher is not clearly better than a

lightweight CNN under the target training regime and objective, CNN-to-CNN feature distillation can lead to systematic negative transfer: the student is pulled toward the teacher rather than beyond.

Takeaway. These three configurations demonstrate a clear pattern for knowledge distillation in Animal Re-ID. In our experiments, matching a smaller Transformer to a larger Transformer preserves retrieval performance but exceeds the memory budget of MCU-class devices, whereas using either a cross-architecture Transformer–CNN pair or a weaker CNN teacher never improves over training the compact CNN directly. In other words, feature-level distillation is helpful only when the teacher both provides stronger embeddings than a lightweight CNN baseline and is architecturally well aligned with the student; otherwise it tends to offer little benefit or even induce negative transfer. Consequently, feature-level distillation alone does not produce a student that is simultaneously accurate and small enough for MCU deployment. Within our experimental setting and under MCU-class resource constraints, the feature-level distillation configurations we explored did not prove sufficient for obtaining a

student that is both accurate and small enough for deployment. This leads us to instead focus on a more structural evaluation of compact architectures and their trade-offs as a path toward further progress on tiny Animal Re-ID models.

3.3 Low-Resolution Input

The distillation experiments above focus on compressing the model size under relatively favourable imaging conditions (inputs resized to $224 \times 224 \times 3$). In realistic MCU deployments, however, the bottleneck is not only model size but also the quality and resolution of the input. To better approximate these conditions, we next study how the same models behave when the input resolution is reduced to MCU-like levels. In practical MCU settings, memory and sensing constraints make it difficult to rely on high-resolution inputs: (i) limited SRAM imposes strict constraints on the intermediate activation memory budget, and (ii) on-board cameras often cannot provide stable, high-quality images.

In all previous experiments we resized images to $224 \times 224 \times 3$ and trained and evaluated all models at this resolution. To simulate a more realistic embedded deployment scenario, we resize all input images across the datasets to $64 \times 64 \times 3$ and investigate whether this lower-resolution setting has a significant impact on model performance. For convenience and fair comparison, we conduct experimental evaluations on three datasets using two teacher models, while keeping all other training and evaluation settings unchanged.

The results are reported in Table 4. Compared with their higher-resolution counterparts, the models generally obtain lower mAP and Top-1/Top-K accuracy under low resolution. This is because the low-resolution input weakens fine-grained discrimination and makes the ranking of candidates less reliable, consistent with the loss of subtle textures and local identity cues at small spatial scales [19, 49]. High-resolution inputs, by retaining richer potentially discriminative details, are more likely to support accurate matching and stable ranked lists [21]. These observations highlight input resolution as a key factor for MCU-ready animal re-identification. We have to keep the input resolution in mind while designing our architecture.

4 Structurally Guided Width-Depth Pruning for Customizing MobileNetV2

Our initial experiments in Section 3 show that, in a constrained hardware setting, knowledge distillation offers only diminishing returns. We also find that reducing the input resolution to 64×64 leads to a significant drop in accuracy across all tested architectures. This degradation indicates that the fine-grained spatial details that standard models are designed to exploit are largely absent in low-resolution inputs. Among the lightweight models, MobileNetV2 stands out as a deployment-friendly baseline. It achieves the best

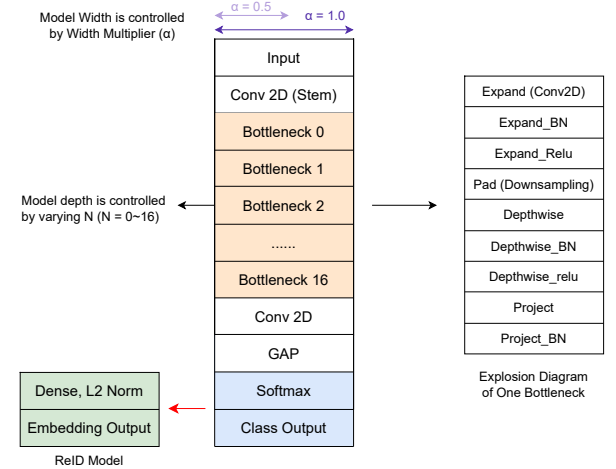


Figure 3: Architecture of the MobileNetV2-based Network with Controllable Depth and Width.

accuracy-complexity trade-off, uses operators supported by common MCU ML runtimes (TensorFlow Lite Micro), however, the standard implementation still exceeds the memory budget of our target MCU and is tuned for high-resolution inputs. Motivated by these observations, we shift our focus from a teacher-based distillation to direct structural optimisation. By systematically scaling the MobileNetV2's structural dimensions, we aim to better match the information content of low-resolution inputs while meeting the stringent memory constraints of the MCU.

4.1 Baseline MobileNetV2 Architecture

We first summarise the features of the baseline MobileNetV2 [36] architecture that are important for our structural depth and width scaling. Our implementation follows the Keras reference configuration [39], with minor changes to accept 64×64 inputs instead of the standard 224×224 . A $64 \times 64 \times 3$ input image is first passed through a 3×3 convolutional stem with a stride of 2, which increases the channel count and reduces the resolution to 32×32 . For convenience, we refer to the number of channels in a feature map as the network width. The rest of the backbone is a simple chain of inverted residual bottleneck blocks. Each block: (1) starts from a relatively narrow feature map (the bottleneck); (2) uses a 1×1 convolution to expand the channels; (3) applies a depthwise 3×3 convolution to capture local spatial patterns; and (4) uses another 1×1 convolution to project back to a narrow bottleneck.

Overall, the MobileNetV2 backbone can be viewed as a sequence of $N = 16$ such blocks arranged from shallow, high-resolution features to deeper, low-resolution features, as shown in Figure 3. In the standard MobileNetV2 design,

Table 4: Teacher performance under high- and low-resolution inputs (blue).

Method	ATRW				FriesianCattle2017				LionData			
	mAP	Top-1	Top-5	Top-10	mAP	Top-1	Top-5	Top-10	mAP	Top-1	Top-5	Top-10
CLIP-ReID (high-res)	58.2	94.6	98.6	99.3	89.0	97.6	100.0	100.0	23.9	29.5	68.9	86.9
CLIP-ReID (low-res)	50.3	92.5	98.8	99.3	73.4	88.2	100.0	100.0	17.7	21.3	50.8	75.4
Few-Shot (high-res)	45.5	87.5	96.5	98.1	84.6	91.8	100.0	100.0	20.3	21.3	53.7	72.1
Few-Shot (low-res)	33.6	73.1	90.6	94.1	59.1	80.0	87.1	92.9	19.3	23.0	50.8	68.9

a global width multiplier scales all channel counts in these blocks, and thus controls the overall model width. This regular “stack of similar blocks” layout is what we build on in Section 4.3: we treat each inverted residual block as a unit that can be kept or removed when we adjust the model *depth* (number of blocks), while the width multiplier controls the channel counts inside each block when we adjust the model *width*.

Because Animal Re-ID is a retrieval task rather than a closed-set classification problem, we replace the final softmax classifier with a metric-learning head that produces a d -dimensional, L_2 -normalised embedding, and we train the model with a triplet loss. This change is confined to the prediction layer and does not alter the backbone, so all width and depth scaling in the following subsections applies directly to the original MobileNetV2 design.

4.2 Reduce the Model Width

Our first question is how far we can narrow the MobileNetV2 backbone before accuracy breaks down. We keep the network topology fixed and adjust only the global width multiplier α , which rescales each layer’s channels from C_i to $\lfloor \alpha C_i \rfloor$ while leaving the block structure unchanged [17, 36, 39]. Therefore, α only changes the channel counts (the network width). The overall block structure remains the same while parameters and FLOPs are reduced [39]. Because our Animal Re-ID datasets are relatively small and inputs are only 64×64 , we first ask how important ImageNet pre-training is compared with changing α . TensorFlow provides ImageNet-pretrained checkpoints down to $\alpha = 0.35$, but not for narrower models. Rather than re-training every candidate on ImageNet (which would be costly), we adopt a realistic setup: architectures with available checkpoints use ImageNet pre-training, while those without are randomly initialised and trained only on the Animal Re-ID data. Concretely, we use pretrained models with $\alpha \in \{0.35, 0.5, 0.75, 1.0\}$ and train scratch models with $\alpha \in \{0.25, 0.35, 0.5\}$.

The results in Table 5 show that pre-training has a much larger effect than width. At $\alpha = 0.35$, ImageNet initialisation raises mAP on ATRW from 11.5 (no pre-training) to 30.7, with gains of roughly 15–25 points across datasets compared to training from scratch. At $\alpha = 0.5$, the pretrained model again outperforms its scratch counterpart by about 18 mAP

on ATRW, with similarly significant improvements observed across the other datasets. In contrast, the scratch model at $\alpha = 0.25$ reaches only 10.1 mAP on ATRW and similarly low scores on the other datasets, performing far below even the narrowest pretrained backbone. Thus, under limited Animal Re-ID data and 64×64 inputs, ImageNet pre-training is far more important for accuracy than moderate width changes, and very narrow models without pre-training are not competitive.

Having established that ImageNet pre-training is more important than moderate width changes, we now ask: among ImageNet-pretrained backbones, how sensitive is Re-ID performance to the choice of width multiplier α under our MCU memory constraints? Because the target platform is memory-limited, we restrict attention to the smaller ImageNet-pretrained MobileNetV2 variants with $\alpha \in \{0.35, 0.5, 0.75, 1.0\}$ and reuse the same metric-learning setup as before. These four models have sizes 6.18 MB, 7.31 MB, 9.89 MB, and 13.24 MB, respectively, so decreasing α yields a simple, monotonic trade-off between width and model size.

As shown in Table 5, our results show that once the backbone is ImageNet-pretrained, the narrow models have similar, and sometimes better performance than the wider ones. Varying α among pretrained models changes mAP by at most a few points, and the narrowest model ($\alpha = 0.35$) often matches or slightly exceeds the wider variants in many datasets. For example, on ATRW, the most challenging dataset, $\alpha = 0.35$ achieves the best mAP (30.7) and Top-1 (66.7), and on the remaining datasets its mAP is usually within a few points of the best configuration with comparable Top-1/Top-5 scores. This suggests that at 64×64 resolution the smallest pretrained MobileNetV2 already has sufficient capacity, so additional width brings limited benefit. Because width scaling shrinks MobileNetV2 from 13.24 MB ($\alpha = 1.0$) to 6.18 MB ($\alpha = 0.35$) with only minor losses in retrieval performance, we adopt the ImageNet-pretrained $\alpha = 0.35$ model as the student backbone for all subsequent experiments and deployment. Intuitively, low-resolution inputs and limited training data mean that the task does not require many distinct feature channels: a narrow pretrained backbone already captures most of the useful variation, so extra width mostly adds redundant capacity rather than improving discrimination.

Table 5: Comparison of ReID performance of MobileNetV2 student models under different width multipliers α .

α	ATRW				FriesianCattle2017				LionData			
	mAP	Top-1	Top-5	Top-10	mAP	Top-1	Top-5	Top-10	mAP	Top-1	Top-5	Top-10
0.25 ¹	10.1	10.4	36.8	54.7	18.5	22.4	49.4	67.1	11.0	11.5	32.8	54.5
0.35 ¹	11.5	16.0	43.9	60.6	20.2	23.5	51.8	71.8	10.8	6.6	32.8	45.9
0.35 ²	30.7	66.7	86.1	91.5	58.9	72.9	94.1	96.5	13.3	14.8	37.7	59.0
0.50 ¹	11.0	10.4	36.8	54.7	24.2	27.1	60.0	75.3	11.0	4.9	34.4	55.7
0.50 ²	28.8	62.0	82.5	87.5	59.2	76.5	92.9	97.6	14.2	14.8	37.7	57.4
0.75 ²	27.1	61.8	80.7	86.8	58.9	92.9	92.9	96.5	13.1	8.2	32.8	65.6
1.00 ²	24.3	55.3	77.6	85.4	57.2	69.4	87.1	90.6	13.0	11.5	36.1	49.2
MPDD												
α	mAP	Top-1	Top-5	Top-10	mAP	Top-1	Top-5	Top-10	mAP	Top-1	Top-5	Top-10
0.25 ¹	3.6	1.9	12.5	20.2	15.5	16.8	53.7	71.1	9.8	12.4	40.4	59.4
0.35 ¹	3.8	2.9	7.7	13.4	15.6	13.7	53.9	72.1	13.5	14.4	48.3	67.9
0.35 ²	30.1	40.4	59.6	78.8	18.8	39.2	73.5	87.0	42.6	67.7	90.4	95.2
0.50 ¹	4.3	4.8	10.6	20.2	15.0	14.7	51.6	71.4	14.6	17.8	52.2	69.1
0.50 ²	29.5	39.4	68.3	76.0	20.0	38.1	74.2	84.7	45.0	63.1	88.6	94.1
0.75 ²	32.5	40.4	65.4	78.8	20.5	35.5	69.8	79.0	47.0	68.0	91.0	95.3
1.00 ²	31.5	37.5	66.3	79.8	21.3	36.7	73.0	83.7	45.7	66.5	91.4	95.3

¹ Trained without pre-trained weights. ² Trained with pre-trained weights.

4.3 Reducing the Model Depth

Having fixed the width multiplier to $\alpha = 0.35$, the backbone still exceeds the memory budget of our embedded platform discussed in Section 2. We therefore next ask how much we can reduce the model depth, i.e. the number of inverted residual bottleneck blocks, while keeping the width multiplier unchanged. We will show that retaining only the first seven out of sixteen blocks yields a strong “knee point” in the accuracy–size trade-off: the model shrinks to 1.97 MB while remaining on the near-optimal mAP plateau, with performance comparable to the best depths on all datasets.

With the width fixed at $\alpha = 0.35$, depth is the other major degree of freedom in the backbone design. Increasing depth adds layers and therefore increases parameters and computation, but it is not clear how much additional depth actually helps Animal Re-ID at low resolution. We therefore investigate whether a shorter prefix of MobileNetV2 can retain most of the Animal Re-ID performance while substantially reducing model size.

To study this, we vary depth in a controlled way while keeping the rest of the architecture and training pipeline fixed. MobileNetV2 is organised as a sequence of inverted residual bottlenecks, so we view the $\alpha = 0.35$ backbone as a chain of 16 standard bottleneck blocks between an initial Stem and a final Head followed by the metric-learning embedding layers (global average pooling, dropout, fully connected, and L_2 normalisation). The Stem, the simplified bottleneck 0, the Head, and the embedding layers are kept fixed

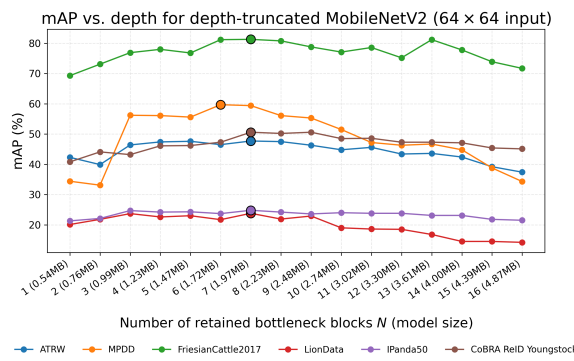
across all variants. These components define the backbone’s input resolution and embedding dimensionality. Keeping them unchanged preserves tensor shapes and maintains full compatibility with our loss functions and evaluation.

Starting from this baseline, we build a set of models that differ only in how many standard bottleneck blocks they contain. For each $N \in \{1, \dots, 16\}$, we keep the first N standard bottlenecks, cut the network after block N , and reuse the original Head and embedding layers on top of its output. As N decreases, the backbone becomes shallower and the model size decrease, while the Stem, bottleneck 0, Head, and embedding layers remain unchanged. This construction isolates the effect of depth: by comparing these variants, we can see how retrieval accuracy degrades as we shorten the backbone and identify depths that offer a good accuracy–size trade-off for deployment.

To evaluate the different backbones, the width multiplier is fixed at $\alpha = 0.35$, and all inputs are resized to 64×64 , matching the constraints of the target MCU deployment. For each value of N , we record mAP and model size. Figure 4 summarises the results. Across all datasets, a similar pattern emerges. For very shallow networks ($N=1\text{--}3$), increasing depth leads to large gains in mAP. Around moderate depths (approximately $N=4\text{--}8$), performance reaches a peak or plateau. Beyond this region, adding further blocks up to the full model ($N=16$) yields little or no improvement and can even slightly degrade mAP on some datasets. This indicates that, under low-resolution 64×64 inputs and narrow width,

Table 6: Performance comparison between Our Method and CLIP-ReID on six public datasets

Method	ATRW				FriesianCattle2017				LionData			
	mAP	Top-1	Top-5	Top-10	mAP	Top-1	Top-5	Top-10	mAP	Top-1	Top-5	Top-10
CLIP-ReID	50.3	92.5	98.8	99.3	73.4	88.2	100.0	100.0	17.7	21.3	50.8	75.4
Our Method	47.7	87.3	95.5	97.2	81.3	87.1	97.6	98.8	23.8	37.7	59.0	67.2
MPDD				IPanda50				CoBRA ReID Youngstock				
Method	mAP	Top-1	Top-5	Top-10	mAP	Top-1	Top-5	Top-10	mAP	Top-1	Top-5	Top-10
CLIP-ReID	60.9	78.8	92.3	96.2	27.5	77.8	94.3	96.7	62.0	93.4	98.6	99.3
Our Method	59.4	73.1	90.4	93.3	24.8	60.0	84.1	93.4	50.6	74.7	94.6	97.3

**Figure 4: mAP with the number of retained bottleneck blocks N for depth-truncated MobileNetV2 backbones.**

the representational capacity of the backbone saturates at moderate depth, and additional layers offer diminishing returns.

Among all depth configurations, $N=7$ emerges as a consistently strong choice. For ATRW, FriesianCattle2017, and CoBRA ReID Youngstock, $N=7$ is at or very near the global optimum, with mAP typically within 1–2 points of the best depth. On MPDD, the maximum mAP occurs at $N=6$, but the curve is flat and performance at $N=7$ is essentially unchanged. For LionData and IPanda50, where overall mAP is lower and the curves are flatter, $N=7$ also lies on the top plateau and is indistinguishable from the best configuration within normal experimental variation. Model size moves in the opposite direction: each additional block increases parameters and Flash usage. Within the $\alpha = 0.35$ family, the full-depth model ($N=16$) occupies about 4.87 MB, whereas $N=7$ uses only 1.97 MB, leading a reduction of nearly 60% while staying on the accuracy plateau across datasets. We therefore regard $N=7$ as a deployment-friendly depth that offers a good balance between retrieval performance and compactness.

This “knee point” at moderate depth can be understood from the interaction between network capacity, resolution, and data scale. When N is too small, the shallow backbone

cannot capture the appearance variation, pose changes, and background clutter inherent to animal re-identification, leading to underfitting and low mAP. As depth increases, the network gains a larger effective receptive field and richer hierarchical features, which improves retrieval. However, with 64×64 inputs and fixed width $\alpha=0.35$, the repeated strided convolutions quickly reduce the spatial resolution of the feature maps. Beyond roughly seven bottleneck blocks, most additional layers operate on very small feature maps and mainly recombine existing coarse features rather than introducing genuinely new information, while still adding parameters. Given the limited amount of training data, this extra capacity is hard to exploit and can even hurt generalisation. The empirical curves in Figure 4 therefore suggest that $N \approx 7$ strikes a good compromise: the backbone is deep enough to model the necessary appearance complexity, but not so deep that its capacity becomes redundant, making it well suited for MCU deployment.

Summary. In this section, we asked two questions for MobileNetV2 under MCU constraints: how narrow and how shallow can the backbone be before Re-ID accuracy breaks down? Our width study showed that ImageNet pre-training matters more than the exact width multiplier: even the smallest pretrained backbone ($\alpha = 0.35$) reaches competitive mAP, making it the best accuracy–size trade-off. Fixing $\alpha = 0.35$, a block-wise depth sweep then revealed a clear knee around $N = 7$ bottleneck blocks, which stays on the near-optimal mAP plateau across datasets while cutting parameters and Flash usage by almost 70% compared with the full-depth $\alpha = 0.35$ network. Compared with the CLIP-ReID teacher, this ultra-lightweight student achieves a strong accuracy–memory balance (Table 6). The model size drops from 477 MB to 1.97 MB (about 242×) while Re-ID performance remains competitive across all six public datasets: our model matches or improves on CLIP-ReID for FriesianCattle2017 and LionData, shows only modest drops on ATRW and MPDD, and exhibits larger but still acceptable degradation on IPanda50 and CoBRA ReID Youngstock. For example, on FriesianCattle2017 our method increases mAP by 7.9

points, indicating that a highly compressed MobileNetV2 can even surpass the teacher in some scenarios. These results suggest that the proposed model preserves most of CLIP-ReID’s retrieval capability under MCU constraints and provides a practical, efficient backbone for embedded Animal Re-ID.

5 Experiment on Arduino

After pruning and compressing the backbone network as described in Section 4, we obtain a final 1.97 MB model ready for deployment on the MCU. This section describes how this trained network is converted into an embedded-ready model through post-training quantisation, conversion into an embedded-ready model format, and deployment on a low-power Arduino platform for on-device evaluation.

5.1 Quantisation and Model Conversion

The final deployment target is an Arduino-class MCU whose inference stack only supports efficient 8-bit integer (INT8) operations and does not execute standard 32-bit floating-point (FP32) operations commonly used in workstations and servers. To run our compact CNN under these constraints, we convert the pretrained FP32 model into a fully integer model and then export it into an embedded-ready format. At a high level, this involves (i) applying post-training quantisation to map weights and activations from FP32 to INT8, and (ii) converting the resulting integer-only model into a deployable MCU model.

We use Post-Training Quantization (PTQ) in TensorFlow Lite, which converts a trained floating-point network into an integer-only inference graph without additional retraining [11, 40]. Given a floating-point tensor $x \in \mathbb{R}$, affine quantisation maps it to an integer tensor $x_q \in \{-128, \dots, 127\}$ [18]. We use per-channel quantisation for convolutional weights to better preserve precision and per-tensor quantisation for activations to maintain computational efficiency [30].

We apply this PTQ scheme to the trained FP32 CNN so that the Arduino runtime can execute it using only 8-bit integer operations. We use the TensorFlow Lite converter with integer-only optimisation to rewrite all layers as INT8-compatible operators and define both network inputs and outputs as 8-bit integers. To choose appropriate scales and zero-points for each tensor, the converter runs on a representative set of 100 randomly sampled training images, preprocessed exactly as during training, and records activation ranges for calibration [40]. The resulting quantised network is serialised into a single .tflite FlatBuffer that can be loaded by the MCU runtime and executed directly on the target Arduino platform, providing a compact, integer-only model suitable for deployment.

After this procedure, all model parameters and activations are converted from 32-bit floating point to 8-bit integers, achieving a compression ratio of over 4×: the model size

is reduced from 1.97 MB (FP32) to approximately 84 KB (INT8). Although the available flash and SRAM would permit somewhat larger models, we observed no consistent accuracy gains from scaling beyond this configuration (Section 4), so we adopt this highly compact variant for all deployments.

5.2 Deployment

After obtaining the quantised model, we deploy it to an Arduino Nano 33 BLE Sense MCU to demonstrate fully on-device inference. The quantized model and a test image are compiled into the firmware as constant arrays, so that all computation runs locally on the device without any external host. The input image is resized to $64 \times 64 \times 3$ and quantised to int8 using the same preprocessing and scaling procedure as in training, ensuring consistency between the training and deployment pipelines. At runtime, the model is executed using TensorFlow Lite for MCUs, which provides a light-weight interpreter and a small pre-allocated memory arena in SRAM for all tensors. During inference, the pre-quantized image array is copied into the model’s input buffer and a single forward pass is performed, producing an int8 feature embedding at the network output.

For analysis and retrieval, this embedding is converted back to a continuous representation using the standard quantitation rule, $\text{real} = (q - \text{zero_point}) \times \text{scale}$, applied element-wise with the scale and zero-point parameters associated with the output tensor. The resulting floating-point feature vector serves as a compact representation of the input image and is used for similarity measurement and recognition in downstream evaluation. Empirically, this deployment pipeline performs stable end-to-end inference on the resource-constrained microcontroller, confirming the practicality of the proposed TinyML model in real embedded environments.

5.3 Data Collection and Evaluation

Our goal in this experiment is to evaluate whether the proposed TinyML model can perform reliable Animal Re-ID when deployed end-to-end on a real MCU. To approximate a realistic deployment scenario, we evaluate the model on a self-collected cattle dataset recorded in the natural grazing environment of in Auckland, New Zealand. In this local data collection effort, we obtained 45 individual cattle identities and 549 images in total. After preprocessing, quality filtering, and manual annotation, the images were split into a training set and an evaluation set using an approximate 80%/20% ratio. The final dataset contains 36 training identities and 9 evaluation identities, corresponding to 448 training images, 65 gallery images, and 36 query images.

For evaluation, we use the same gallery-query protocol described earlier: identities are split into a gallery set (reference images) and a query set (images to be identified). Gallery

Table 7: Server and Arduino performance.

Method	mAP	Top-1	Top-5	Top-10	Model Size
Cluster	50.1	61.1	86.1	94.4	1.79 MB
Arduino	45.6	61.1	96.1	91.7	84 KB

images are passed through the on-device model to extract embeddings, which are stored on the Arduino as a reference database. Each query image is then processed to obtain its embedding and matched to the gallery via nearest-neighbour retrieval on the device. To assess the impact of quantisation and deployment, we compare two settings on the same splits: *Cluster*, the original FP32 model run on a compute cluster as an upper bound, and *Arduino*, the quantised INT8 model running entirely on the Nano 33 BLE Sense, with both inference and matching on the MCU.

The results in Table 7 show how much recognition performance is preserved when moving from the floating-point cluster model to the heavily compressed, integer-only MCU model. The cluster model provides the reference performance in FP32. When deployed on the Arduino, the quantised model is compressed from 1.79 MB to only 84 KB, yet it is able to retain most of the Animal Re-ID capability. The mAP decreases moderately (50.1 to 45.6), indicating a small loss in ranking quality, which is consistent with the small numerical changes introduced when compressing the model to 8-bit integers. However, the Top-1 accuracy remains identical at 61.1, showing that the top prediction is correct at the same rate in both settings, and the Top-5 and Top-10 accuracies fluctuate only slightly while staying within a high-performance range. These results indicate that the proposed quantisation and deployment pipeline can reduce the model size by more than an order of magnitude while preserving comparable Animal Re-ID performance.

5.4 Fine Tuning

We have seen that training a model from scratch on our self-collected cattle dataset can yield good performance. However, this setup implicitly assumes that it is always possible to gather a large number of images and train a new model for every deployment site. In practice, this is rarely feasible: gathering and annotating hundreds of images per animal is time-consuming, requires expert effort, and demands compute resources that may not be available in the field. At the same time, there are several public Animal Re-ID datasets. For example, the FriesianCattle2017 dataset also contains cattle. This naturally raises the question of whether we can reuse a model trained on such public data and adapt it to a new site with only a small amount of local data.

However, training on a public dataset and then deploying the model as-is at a new site often does not work well. Public datasets and real deployment environments can differ



(a) Friesiancattle2017

(b) Collected Cattle Image

Figure 5: Cattle from different regions.**Table 8: Performance under different fine-tuning**

Method	mAP	Top-1	Top-5	Top-10
No Fine-tuning	45.0	72.2	88.9	94.4
Fine-tuned (few-shot)	47.8	75.0	88.9	97.2
Training from scratch (new data)	50.1	61.1	86.1	94.4

substantially. As illustrated in Figure 5, cattle from different regions are photographed under different lighting and weather conditions, with distinct backgrounds, ground surfaces, and camera viewpoints. In addition, the animals themselves may look different due to age, body condition, feeding practices, or surface contamination such as mud or partial occlusion [5, 6, 33, 42]. These differences create a domain shift between the source dataset and the target deployment site [52]. If we train only on the public dataset and apply the model directly to our collected images, performance drops because the model has never seen the visual characteristics of the new environment. This is shown in Table 8.

To bridge this gap without collecting a large new dataset, we adopt a data-efficient fine-tuning strategy. We first train the model on a public dataset to learn a general animal re-identification representation and save the resulting weights. When adapting to our collected data, we reload this pre-trained model, freeze the backbone network, and fine-tune only the final embedding layer using the target images. During this stage, we use only a very small amount of new data, typically two to three images per animal identity. This preserves the generic features learned from the source domain, allows the last layer to adjust to the new site, and greatly reduces annotation and computation compared with training from scratch.

Table 8 compares three strategies on the collected dataset. The No fine-tuning setting applies the model trained on the public dataset directly to Cornwall Park, with no adaptation. The Fine-tuned (few-shot) setting uses the same pre-trained model but fine-tunes only the embedding layer with three images per identity. The Training from scratch (new data) setting corresponds to the model trained solely on the collected data, without using the public dataset. The results show that few-shot fine-tuning consistently improves performance over the no-fine-tuning baseline: both mAP and Top-1 increase when a small number of collected data images is used for adaptation. At the same time, the fine-tuned model

remains competitive with the model trained from scratch, despite using far fewer local images and much less computation. In particular, the few-shot model attains the highest Top-1 accuracy, while its mAP stays close to the from-scratch upper bound. Overall, this indicates that the proposed fine-tuning strategy provides a practical, data-efficient way to adapt animal re-identification models to new deployment sites without full retraining.

6 Discussion

This paper presents an initial step toward Animal Re-ID on MCUs, but there are several limitations we'd like to discuss here.

First, our treatment of low-resolution inputs is somewhat idealised. Most experiments use images that are downsampled and resized to $64 \times 64 \times 3$ from public datasets or locally collected smartphone photos. In practice, Arduino-class camera modules introduce their own distortions and noise characteristics (e.g., colour shifts, limited dynamic range, motion blur, compression artefacts) that we do not explicitly model in this work. Our focus here is on understanding whether an MCU-scale model can reliably handle low-resolution inputs and tight memory budgets. A more detailed study of robustness across different embedded camera pipelines is complementary to this goal and forms a natural direction for future on-device experiments.

Second, at the system level, our current system does not yet offer a fully automated end-to-end pipeline. Deploying the model still involves several planned manual steps before exporting the quantised model to the microcontroller. As a result, we do not target a single, plug-and-play pre-trained network that works “out of the box” across all farms or environments. Some additional data collection and light site-specific tuning are still expected. Automating more of this process would further improve usability.

Our system currently serves as a feasibility study and architectural starting point on the path to practical deployments. Building on this foundation, future work can broaden on-device experiments under realistic embedded imaging conditions and integrate the method into a more automated data handling and adaptation pipeline.

7 Related Work

Knowledge distillation. Knowledge distillation (KD) transfers the “soft” predictions of a large teacher into a smaller student and is widely used for compressing deep models while retaining accuracy [15]. In Re-ID, KD has been used to build lighter person and object Re-ID models by distilling similarity structure or uncertainty-aware features from strong teachers [20, 46]. TinyML surveys likewise highlight KD, alongside quantization and pruning, as a core tool for adapting networks to microcontroller-class hardware [14].

In our setting, we ask whether KD can effectively shrink GPU-scale Animal Re-ID models down to MCU scale under low-resolution inputs and constrained memory. We evaluate several routes and find that conventional feature-level KD yields only limited gains over directly trained compact CNNs. This motivates our emphasis on structure-guided width-depth scaling and quantization as primary levers for MCU-level Animal Re-ID.

Neural Architecture Search. A complementary, bottom-up line of work addresses resource constraints by explicitly designing lightweight backbones and scaling them under accuracy-efficiency trade-offs. MobileNetV2, for example, uses inverted residual blocks with linear bottlenecks and depthwise separable convolutions to reduce parameters and multiply-add operations while maintaining strong accuracy across a range of model sizes [36]. EfficientNet builds on this idea by jointly scaling network depth, width, and input resolution with a single compound coefficient, combined with a NAS-derived baseline, to produce model families tuned to different compute budgets [38]. TinyML-oriented frameworks such as MCUNet go further by co-designing constrained neural architectures (TinyNAS) and memory-efficient inference engines (TinyEngine) to achieve ImageNet-scale inference on MCUs with only tens to hundreds of kilobytes of memory [27]. More generally, MCU-oriented NAS formulations hard-code on-chip SRAM, flash capacity, and latency into the search objective, yielding architectures whose depth, width, and activation footprint are tightly fitted to specific MCU targets. Recent work such as MCUNetV2 and hardware-aware NAS frameworks (e.g., Once-for-All, FBNet) shows that such device-specific search can significantly improve accuracy-efficiency trade-offs on tiny devices [7, 47]. These structurally guided designs provide a useful foundation for efficient vision on edge devices, but they mainly target classification tasks and typically operate at larger model scales and more relaxed memory budgets than those required for MCU-based Animal Re-ID.

8 Conclusion

We take a first step toward running Animal Re-ID directly on MCU-class devices. Starting from the gap between GPU-oriented models and MCU constraints, we explore architecture scaling and quantisation, arriving at a tiny INT8 CNN that fits within strict memory limits while maintaining competitive accuracy on both public benchmarks and a real-world cattle deployment. Building on this backbone, we show that a simple few-shot fine-tuning scheme can adapt the model to new sites using only a small number of images per animal, avoiding the need to train from scratch at each location. Together, these results outline a practical recipe for Animal Re-ID on edge and point toward future systems that perform monitoring entirely on low-power edge hardware.

References

[1] Sabbir Ahmed, Abdullah Al Arafat, Deniz Najafi, Akhlak Mahmood, Mamshad Nayeem Rizve, Mohaiminul Al Nahian, Ranyang Zhou, Shaahin Angizi, and Adnan Siraj Rakin. 2025. DeepCompress-ViT: Rethinking Model Compression to Enhance Efficiency of Vision Transformers at the Edge. In *Proceedings of the Computer Vision and Pattern Recognition Conference*. 30147–30156.

[2] Sungsoo Ahn, Shell Xu Hu, Andreas Damianou, Neil D Lawrence, and Zhenwen Dai. 2019. Variational information distillation for knowledge transfer. In *Proceedings of the IEEE/CVF conference on computer vision and pattern recognition*. 9163–9171.

[3] Norah N Alajlan and Dina M Ibrahim. 2022. TinyML: Enabling of inference deep learning models on ultra-low-power IoT edge devices for AI applications. *Micromachines* 13, 6 (2022), 851.

[4] William Andrew, Colin Greatwood, and Tilo Burghardt. 2017. Visual localisation and individual identification of holstein friesian cattle via deep learning. In *Proceedings of the IEEE international conference on computer vision workshops*. 2850–2859.

[5] Sara Beery, Grant Van Horn, and Pietro Perona. 2018. Recognition in terra incognita. In *Proceedings of the European conference on computer vision (ECCV)*. 456–473.

[6] Yannick Burkard, Emanuele Francazi, Edward Lavender, Tina Dubach, Sabrina Wehrli, Jakob Brodesen, Michele Volpi, Marco Baity Jesi, and Helen Moor. 2024. Automated single species identification in camera trap images: architecture choice, training strategies, and the interpretation of performance metrics. (2024).

[7] Han Cai, Chuang Gan, Tianzhe Wang, Zhekai Zhang, and Song Han. 2019. Once-for-all: Train one network and specialize it for efficient deployment. *arXiv preprint arXiv:1908.09791* (2019).

[8] Nkosikhona Dlamini and Terence L Van Zyl. 2020. Automated identification of individuals in wildlife population using siamese neural networks. In *2020 7th international conference on soft computing & machine intelligence (ISCFMI)*. IEEE, 224–228.

[9] Alexey Dosovitskiy. 2020. An image is worth 16x16 words: Transformers for image recognition at scale. *arXiv preprint arXiv:2010.11929* (2020).

[10] Jin Gao, Shubo Lin, Shaoru Wang, Yutong Kou, Zeming Li, Liang Li, Congxuan Zhang, Xiaoqin Zhang, Yizheng Wang, and Weiming Hu. 2025. An Experimental Study on Exploring Strong Lightweight Vision Transformers via Masked Image Modeling Pre-training. *International Journal of Computer Vision* 133, 7 (2025), 3918–3950.

[11] Google AI Edge Team. 2024. Post-training quantization. Google AI Edge LiteRT Documentation. https://ai.google.dev/edge/liter/models/post_training_quantization Accessed: 2025-11-21.

[12] Xi Guo, Yufeng Chen, Yu Guan, Hongfang Wang, Tianming Wang, Jianping Ge, and Lei Bao. 2025. Individual identification of wild raptors using a deep learning approach: A case study of the white-tailed eagle. *Ecological Informatics* (2025), 103379.

[13] Zhimin He, Jiangbo Qian, Diquan Yan, Chong Wang, and Yu Xin. 2023. Animal re-identification algorithm for posture diversity. In *ICASSP 2023-2023 IEEE International Conference on Acoustics, Speech and Signal Processing (ICASSP)*. IEEE, 1–5.

[14] Soroush Heydari and Qusay H Mahmoud. 2025. Tiny machine learning and on-device inference: A survey of applications, challenges, and future directions. *Sensors* 25, 10 (2025), 3191.

[15] Geoffrey Hinton, Oriol Vinyals, and Jeff Dean. 2015. Distilling the knowledge in a neural network. *arXiv preprint arXiv:1503.02531* (2015).

[16] Md Imtiaz Hossain, Sharmin Akhter, Choong Seon Hong, and Eui-Nam Huh. 2025. Single teacher, multiple perspectives: Teacher knowledge augmentation for enhanced knowledge distillation. In *The Thirteenth International Conference on Learning Representations*.

[17] Andrew G Howard, Menglong Zhu, Bo Chen, Dmitry Kalenichenko, Weijun Wang, Tobias Weyand, Marco Andreetto, and Hartwig Adam. 2017. Movenet: Efficient convolutional neural networks for mobile vision applications. *arXiv preprint arXiv:1704.04861* (2017).

[18] Benoit Jacob, Skirmantas Kligys, Bo Chen, Menglong Zhu, Matthew Tang, Andrew Howard, Hartwig Adam, and Dmitry Kalenichenko. 2018. Quantization and training of neural networks for efficient integer-arithmetic-only inference. In *Proceedings of the IEEE conference on computer vision and pattern recognition*. 2704–2713.

[19] Jiening Jiao, Wei-Shi Zheng, Ancong Wu, Xiatian Zhu, and Shaogang Gong. 2018. Deep low-resolution person re-identification. In *Proceedings of the AAAI conference on artificial intelligence*, Vol. 32.

[20] Xin Jin, Cuiling Lan, Wenjun Zeng, and Zhibo Chen. 2020. Uncertainty-aware multi-shot knowledge distillation for image-based object re-identification. In *Proceedings of the AAAI Conference on Artificial Intelligence*, Vol. 34. 11165–11172.

[21] Xiao-Yuan Jing, Xiaoke Zhu, Fei Wu, Xinge You, Qinglong Liu, Dong Yue, Ruimin Hu, and Baowen Xu. 2015. Super-resolution person re-identification with semi-coupled low-rank discriminant dictionary learning. In *Proceedings of the IEEE conference on computer vision and pattern recognition*. 695–704.

[22] Emmanuel Kabuga, Izzy Langley, Monica Arso Civil, John Measey, Bubacarr Bah, and Ian Durbach. 2024. Similarity learning networks uniquely identify individuals of four marine and terrestrial species. *Ecosphere* 15, 10 (2024), e70012. doi:10.1002/ecs2.70012

[23] Taylor L Kaltenbach, Jeffrey C Mosley, Lance B McNew, and Jared T Beaver. 2025. Can edge AI mitigate environmental effects on camera trap performance? *Wildlife Society Bulletin* (2025), e1598.

[24] Zhenglun Kong, Dongkuan Xu, Zhengang Li, Peiyan Dong, Hao Tang, Yanzhi Wang, and Subhabrata Mukherjee. 2025. AutoViT: Achieving Real-Time Vision Transformers on Mobile via Latency-aware Coarse-to-Fine Search. *International Journal of Computer Vision* (2025), 1–17.

[25] Shuyuan Li, Jianguo Li, Hanlin Tang, Rui Qian, and Weiyao Lin. 2019. ATRW: a benchmark for Amur tiger re-identification in the wild. *arXiv preprint arXiv:1906.05586* (2019).

[26] Siyuan Li, Li Sun, and Qingli Li. 2023. Clip-reid: Exploiting vision-language model for image re-identification without concrete text labels. In *Proceedings of the AAAI conference on artificial intelligence*, Vol. 37. 1405–1413.

[27] Ji Lin, Wei-Ming Chen, Yujun Lin, Chuang Gan, Song Han, et al. 2020. Mcunet: Tiny deep learning on iot devices. *Advances in neural information processing systems* 33 (2020), 11711–11722.

[28] Amir Moslemi, Anna Briskina, Zubeka Dang, and Jason Li. 2024. A survey on knowledge distillation: Recent advancements. *Machine Learning with Applications* 18 (2024), 100605.

[29] Margarita Mulero-Pázmány, Sandro Hurtado, Cristóbal Barber-González, María Luisa Antequera-Gómez, Francisco Díaz-Ruiz, Raimundo Real, Ismael Navas-Delgado, and José F Aldana-Montes. 2025. Addressing significant challenges for animal detection in camera trap images: a novel deep learning-based approach. *Scientific Reports* 15, 1 (2025), 16191.

[30] Markus Nagel, Marios Fournarakis, Rana Ali Amjad, Yelysei Bondarenko, Mart Van Baalen, and Tijmen Blankevoort. 2021. A white paper on neural network quantization. *arXiv preprint arXiv:2106.08295* (2021).

[31] Maarten Perneel, Ines Adriaens, Jan Verwaeren, and Ben Aernouts. 2025. Dynamic Multi-Behaviour, Orientation-Invariant Re-Identification of Holstein-Friesian Cattle. *Sensors* 25, 10 (2025), 2971.

[32] Alec Radford, Jong Wook Kim, Chris Hallacy, Aditya Ramesh, Gabriel Goh, Sandhini Agarwal, Girish Sastry, Amanda Askell, Pamela Mishkin, Jack Clark, et al. 2021. Learning transferable visual models from natural

language supervision. In *International conference on machine learning*. PMLR, 8748–8763.

[33] Mohammad Mehdi Rastikerdar, Jin Huang, Hui Guan, and Deepak Ganesan. 2024. In-Situ Fine-Tuning of Wildlife Models in IoT-Enabled Camera Traps for Efficient Adaptation. *arXiv preprint arXiv:2409.07796* (2024).

[34] Partha Pratim Ray. 2022. A review on TinyML:: State-of-the-art and prospects. (2022).

[35] Shaibal Saha and Lanyu Xu. 2025. Vision transformers on the edge: A comprehensive survey of model compression and acceleration strategies. *Neurocomputing* (2025), 130417.

[36] Mark Sandler, Andrew Howard, Menglong Zhu, Andrey Zhmoginov, and Liang-Chieh Chen. 2018. Mobilenetv2: Inverted residuals and linear bottlenecks. In *Proceedings of the IEEE conference on computer vision and pattern recognition*. 4510–4520.

[37] Moritz Scherer, Fabian Sidler, Michael Rogenmoser, Michele Magno, and Luca Benini. 2022. Widetvision: A low-power, multi-protocol wireless vision platform for distributed surveillance. In *2022 18th International Conference on Wireless and Mobile Computing, Networking and Communications (WiMob)*. IEEE, 394–399.

[38] Mingxing Tan and Quoc Le. 2019. Efficientnet: Rethinking model scaling for convolutional neural networks. In *International conference on machine learning*. PMLR, 6105–6114.

[39] Keras Team. [n. d.]. MobileNet, MobileNetV2, and MobileNetV3. Keras 3 API documentation. <https://keras.io/api/applications/mobilenet/> Accessed: 2025-11-21.

[40] TensorFlow Authors. 2022. Post-training quantization. TensorFlow Model Optimization Guide. https://www.tensorflow.org/model_optimization/guide/quantization/post_training Accessed: 2025-11-21.

[41] Hugo Touvron, Matthieu Cord, Matthijs Douze, Francisco Massa, Alexandre Sablayrolles, and Hervé Jégou. 2021. Training data-efficient image transformers & distillation through attention. In *International conference on machine learning*. PMLR, 10347–10357.

[42] Devis Tuia, Benjamin Kellenberger, Sara Beery, Blair R Costelloe, Silvia Zuffi, Benjamin Risse, Alexander Mathis, Mackenzie W Mathis, Frank Van Langevelde, Tilo Burghardt, et al. 2022. Perspectives in machine learning for wildlife conservation. *Nature communications* 13, 1 (2022), 792.

[43] Delia Velasco-Montero, Jorge Fernández-Berni, Ricardo Carmona-Galán, Ariadna Sanglas, and Francisco Palomares. 2024. Reliable and efficient integration of AI into camera traps for smart wildlife monitoring based on continual learning. *Ecological Informatics* 83 (2024), 102815.

[44] Oscar Wahltinez and Sarah J Wahltinez. 2024. An open-source general purpose machine learning framework for individual animal re-identification using few-shot learning. *Methods in Ecology and Evolution* 15, 2 (2024), 373–387.

[45] Le Wang, Rizhi Ding, Yuanhao Zhai, Qilin Zhang, Wei Tang, Nanning Zheng, and Gang Hua. 2021. Giant panda identification. *IEEE Transactions on Image Processing* 30 (2021), 2837–2849.

[46] Ancong Wu, Wei-Shi Zheng, Xiaowei Guo, and Jian-Huang Lai. 2019. Distilled person re-identification: Towards a more scalable system. In *Proceedings of the IEEE/CVF Conference on Computer Vision and Pattern Recognition*. 1187–1196.

[47] Bichen Wu, Xiaoliang Dai, Peizhao Zhang, Yanghan Wang, Fei Sun, Yiming Wu, Yuandong Tian, Peter Vajda, Yangqing Jia, and Kurt Keutzer. 2019. Fbnet: Hardware-aware efficient convnet design via differentiable neural architecture search. In *Proceedings of the IEEE/CVF conference on computer vision and pattern recognition*. 10734–10742.

[48] Zhendong Yang, Zhe Li, Ailing Zeng, Zexian Li, Chun Yuan, and Yu Li. 2024. Vitkd: Feature-based knowledge distillation for vision transformers. In *Proceedings of the IEEE/CVF Conference on Computer Vision and Pattern Recognition*. 1379–1388.

[49] Guoqing Zhang, Yuhao Chen, Weisi Lin, Arun Chandran, and Xuan Jing. 2021. Low resolution information also matters: Learning multi-resolution representations for person re-identification. *arXiv preprint arXiv:2105.12684* (2021).

[50] Liang Zheng, Liyue Shen, Lu Tian, Shengjin Wang, Jingdong Wang, and Qi Tian. 2015. Scalable person re-identification: A benchmark. In *Proceedings of the IEEE international conference on computer vision*. 1116–1124.

[51] Yuji Zhong, Xiao Li, Jiangjian Xie, and Junguo Zhang. 2023. A light-weight automatic wildlife recognition model design method mitigating shortcut learning. *Animals* 13, 5 (2023), 838.

[52] Kaiyang Zhou, Ziwei Liu, Yu Qiao, Tao Xiang, and Chen Change Loy. 2022. Domain generalization: A survey. *IEEE transactions on pattern analysis and machine intelligence* 45, 4 (2022), 4396–4415.